2004

Sediment-magnetic Signature of Land-use and Drought as Recorded in Lake Sediment from South-central Minnesota, U.S.A.

Christoph E. Geiss
Trinity College

Subir K. Banerjee
University of Minnesota - Twin Cities

Philip Camill
Carleton College

Charles E. Umbanhowar
St. Olaf College

Available online at www.sciencedirect.com

SCIENCE DIRECT®

Quaternary Research 62 (2004) 117–125

QUATERNARY RESEARCH

www.elsevier.com/locate/yqres

Sediment-magnetic signature of land-use and drought as recorded in lake sediment from south-central Minnesota, USA

Christoph E. Geiss[a,*], Subir K. Banerjee[b], Phil Camill[c], Charles E. Umbanhowar Jr.[d]

[a]*Department of Physics, Trinity College, Hartford, CT 06106, United States*
[b]*Department of Geology and Geophysics, University of Minnesota, Minneapolis, MN 55455, United States*
[c]*Department of Biology, Carleton College, Northfield, MN 55057, United States*
[d]*Department of Biology, St. Olaf College, Northfield, MN 55057, United States*

Received 20 August 2003

Abstract

Sediment magnetic properties of a short core from Sharkey Lake, MN, record the effects of Euroamerican settlement and climate change over the last 150 yr. The onset of European-style farming led to increased erosion, reflected in high values of concentration-dependent parameters such as magnetic susceptibility (κ), Isothermal Remanent Magnetization (IRM), and Anhysteretic Remanent Magnetization (ARM). These high values are only partially due to increased supply of terrigenous material to the lake, and recent sediment contains an additional component of authigenic fine (single-domain) magnetite, most likely magnetosomes from magnetotactic bacteria. High organic productivity in the lake during the 1920s to 1940s drought increased this authigenic component resulting in highly magnetic fine-grained sediment. A comparison with older Holocene sediment from the same lake shows that, over time, most of the fine magnetic signal is lost after deposition, leading to decreases in magnetization and a bimodal grain size distribution of ultrafine, superparamagnetic grains and coarser multidomain particles, evident from measurements of ARM/IRM ratios, hysteresis measurements, and low-temperature analyses. The effects of dissolution and the superposition of climate and land-use signals complicate the use of recent sediments as modern analogs for sediment magnetic analyses.

Keywords: Sediment magnetism; Holocene; Limnology; Drought; Reductive dissolution; Magnetotactic bacteria

Introduction

In recent years, sediment-magnetic investigations have played an increasingly important role in reconstructing paleoenvironmental and paleoclimatic change from continental and marine records. Multi-proxy studies that include sediment-magnetic analyses have successfully reconstructed late Pleistocene and Holocene climate variations (e.g., Oldfield et al., 2003; Rosenbaum et al., 1996), have clarified sediment provenance (Reynolds et al., 1997), or established the fire history of a watershed (Gedye et al., 2000).

Sediment-magnetic parameters are easily measured and allow for the rapid construction of high-resolution records of paleoclimate independent from other paleoclimate proxies, such as pollen or geochemistry. They are, however, no direct recorder of climate or environmental change. Interpretation of magnetic parameters in such terms requires identification of the underlying processes that influence the input, distribution, preservation, or neoformation of the minerals that make up the magnetic component of the sediment. Research described in this paper helps to improve the interpretation of sediment-magnetic parameters by comparing them to known climatic or environmental changes.

Geiss et al. (2003) studied several lakes along the prairie-forest ecotone in Minnesota to determine the processes that

* Corresponding author. Department of Physics, Trinity College, 300 Summit Street, Hartford, CT 06106.
E-mail addresses: christoph.geiss@trincoll.edu (C.E. Geiss), banerjee@umn.edu (S.K. Banerjee), pcamill@carleton.edu (P. Camill), ceumb@stolaf.edu (C.E. Umbanhowar).

0033-5894/$ - see front matter © 2004 University of Washington. All rights reserved.
doi:10.1016/j.yqres.2004.06.009

link Holocene paleoenvironmental change to variations in sediment magnetic properties, to develop a model that allows one to interpret these variations in terms of paleoclimate, and to reconstruct high-resolution paleoclimate records. In that study, we found that mid-Holocene drought (e.g., Wright, 1992) led to increased deposition of clastic material either through eolian deposition or soil erosion, causing high concentrations of magnetic minerals, combined with a shift in grain size toward coarse multi-domain (MD) magnetic grains. Sediment deposited during humid periods is characterized by low concentrations of clastic material, leading to low concentrations of magnetic minerals, combined with a shift to fine-grained, single-domain (SD) magnetic particles, which are likely of allochthonous origin.

In this paper, we relate variations, observed in a multi-proxy short-core record from Sharkey Lake in south-central Minnesota (Fig. 1), to known changes in land use and climate. The short-core data and its comparison with data from the Holocene (Geiss et al., 2003) will allow us to answer the following main questions:

- To which degree can modern sediment, which records the combined influences of climate and anthropogenic land-use change, yield paleoclimatic information and serve as a modern analog for older records? Modern analog studies are common in the reconstruction of paleoclimate, but their application is complicated by the fact that 20th century drought events appear to be less severe than mid-Holocene droughts (Laird et al., 1996; Stokes and Swinehart, 1997) and that any anthropogenic signal of Euroamerican settlement in the mid-19th century coincides with climatic shifts associated with the end of the Little Ice Age.
- How do the effects of long-term dissolution of Fe-oxides, which occur not only in lacustrine or marine sediments but also loess paleosol sequences, affect the sediment magnetic signal and its interpretation?
- Are sediment magnetic data from short cores useful aids in the interpretation of older magnetic records?

Methods

In March 2002, we collected a core, 150 cm long, from the SE basin of Sharkey Lake (Fig. 1) with a piston corer 7.6 cm (3 in) in diameter. The extremely soft sediment was extruded in the field and immediately subsampled into plastic containers. For magnetic analyses, the sediment was packed into weakly diamagnetic plastic cubes (volume = 5.28 cm^3). All samples were stored moist in resealable plastic bags at approximately 4°C. Water content and abundance of carbonates and organic matter were obtained from loss-on-ignition (LOI) measurements (Dean, 1974). Biogenic silica (Conley, 1998) was measured to estimate organic productivity and to determine, in combination with LOI analyses, the abundance of clastic material. An age chronology was established using a modification of the ^{210}Pb dating method of Eakins and Morrison (1978) (Camill, 1999, Camill et al., 2001).

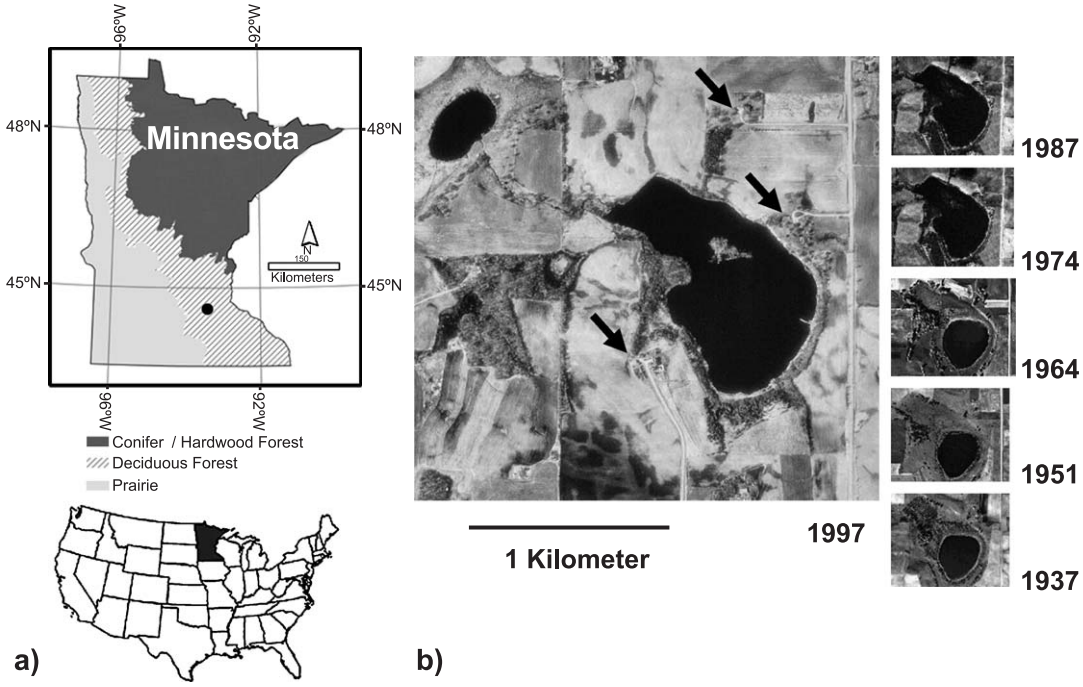

Figure 1. (a) Map of Minnesota, showing the location of Sharkey Lake (SHA) and the major vegetation zones (modified from MN Dept. of Nat. Resources). (b) Series of aerial photographs showing changes in lake levels since 1937 (source: Agricultural Stabilization and Conservation Service, St. Paul, MN). Arrows in 1997 photo show locations of recent building projects. The coring site is in the deep southern basin.

Particle emission was counted for 24 h with an alpha spectrometer (Ortec, Oak Ridge, TN), and the age profile (Fig. 2, Table 1) was determined using a Constant Rate of Supply (CRS) model according to the method of Binford (1990). Sedimentation rates for sediment deposited before the onset of European settlement were estimated from the position of the *Ambrosia* rise and by AMS ^{14}C dates obtained from cores taken in 2001 (Table 1 in Geiss et al., 2003).

The magnetic mineralogy of the samples was characterized through thermal demagnetization of saturation remanence acquired at low temperatures (10 K) to observe thermal demagnetization behavior (e.g., Hunt et al., 1995) and mineral-specific phase transitions (e.g., Housen et al., 1996; Rochette et al., 1990; Verwey et al., 1947). These low-temperature analyses were made with a Quantum Design MPMS 5s magnetometer, which has a sensitivity of 1×10^{-11} Am^2, resulting in errors of less than 1%. Isothermal Remanent Magnetization (IRM) acquisition, measured in magnetizing fields between 1.3 and 1300 mT, was used to characterize the coercivity distributions of all samples and to aid in mineral identification and indirect grain size determination. We calculated hard IRM (HIRM = $IRM_{1000\ mT} - IRM_{320\ mT}$) to track absolute concentrations of high-coercivity minerals such as hematite and goethite, while S-ratios measured in backfields of 100 mT ($S_{100} = -IRM_{-100\ mT}/IRM_{1000\ mT}$) were used to track the relative abundance of these minerals.

The concentration of magnetic minerals was estimated by measuring low-field magnetic susceptibility (κ), Isothermal Remanent Magnetization (IRM), and saturation magnetization (J_S). κ was measured on a Kappabridge KLY-2. To correct for the presence of para- or diamagnetic minerals, we calculated ferrimagnetic susceptibility by subtracting the high field slope (κ_{hf}) of hysteresis loop measurements (para- or dia-magnetic susceptibility contributions) from low-field susceptibility ($\kappa_{ferri} = \kappa - \kappa_{hf}$). IRM was acquired in a DC field (B = 100 mT) of an electromagnet, while J_S was estimated from slope-corrected hysteresis loops measured on a MicroVSM (Princeton Measurement Corp.) at a maximum field of 1300 mT.

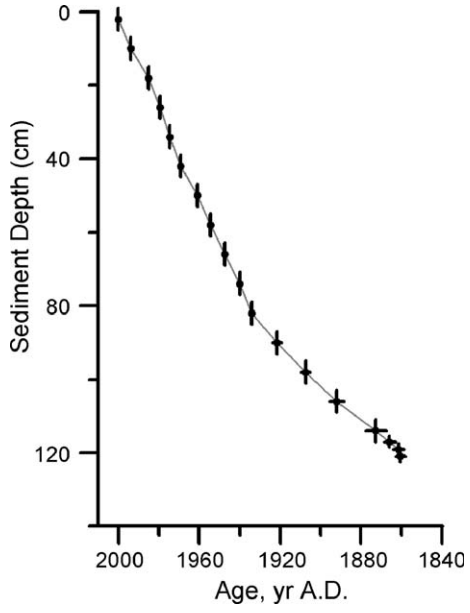

Figure 2. Depth age curve for Sharkey Lake short core (SHA 02-SC) based on ^{210}Pb measurements. For additional information, see Table 1 and text.

The relative abundance of single-domain (SD) particles was estimated from ARM/IRM ratios. Anhysteretic Remanent Magnetization (ARM) was acquired in a peak AF field of 100 mT and a bias field of 50 μT with a D-Tech D-2000 AF demagnetizer. The relative abundance of superparamagnetic particles was estimated from κ_{ferri}/J_S ratios and from thermal demagnetization curves of saturation remanence acquired at 10 K. Hysteresis parameters (Day et al., 1977) were also used to establish general trends in bulk magnetic grain size.

All remanence parameters were measured using a cryogenic magnetometer (2G model 760-R). The magnetometer has a sensitivity of 2×10^{-11} Am^2 leading to errors of approximately 1% for ARM, ARM/IRM, and HIRM measurements and errors better than 0.01% for IRM. The Kappabridge KLY-2 has a sensitivity of 4×10^{-8} SI, resulting in an error better than 1% for κ. Error estimates for hysteresis parameters are more problematic because they depend on the sensitivity of the instrument (2×10^{-8} Am^2) as well as the algorithm used to measure and evaluate hysteresis loops. We conservatively estimate the error associated with κ_{hf} and J_S at 5%, resulting in a maximum error for κ_{ferri} of approximately 6% and an approximate error of 10% for κ_{ferri}/J_S.

The recent precipitation history of Minnesota (MN) was estimated from various sources. Precipitation data are available for Fort Snelling, MN (Fig. 3a) starting in 1837 (MN Dept. of Natural Resources State Climatology Office, personal communication 2003), which were compared to historic streamflow data for the Minnesota (Fig. 3c) and Mississippi (Fig. 3b) rivers (U.S. Geological Survey, 2003). The two streamflow records average over large parts of the state and show a smoother climate signal than the Ft. Snelling record. All three records, however, display the same climatic trends. We use the Mississippi discharge record as a precipitation proxy for Sharkey Lake because the Minnesota River record is shorter and incomplete between A.D. 1920 and 1930. Aerial photographs (Fig. 1b) taken between A.D. 1937 and A.D. 1997 were used to establish lake-level variations and changes in land use through time.

Site description

Sharkey Lake is a small (700 × 400 m) glacial lake in the Altamont stagnation moraine 5 miles west of New Market, MN (44°35′39″ N, 093°24′49″ W) (Hobbs and

Table 1
^{210}Pb Dating of core SHA 02-SC

Top interval depth (cm)	Bottom interval depth (cm)	Total ^{210}Pb activity (dpm/g)	Standard deviation of activity	Date at base of interval (yr A.D.)	Standard deviation of date (yr)
0	4	49.10	2.45	2000	0.46
8	12	23.37	1.34	1994	0.52
16	20	15.32	0.83	1985	0.54
24	28	6.44	0.43	1980	0.50
32	36	5.73	0.42	1975	0.53
40	44	5.06	0.33	1969	0.55
48	52	5.93	0.43	1961	0.68
56	60	4.64	0.35	1955	0.57
64	68	4.85	0.34	1947	0.64
72	76	4.57	0.31	1940	0.61
80	84	3.49	0.28	1934	0.65
88	92	4.15	0.35	1922	1.38
96	100	3.31	0.29	1907	1.43
104	108	3.05	0.27	1892	2.44
112	116	2.74	0.26	1873	3.50
116	118	2.86	0.27	1866	1.93
118	120	2.41	0.22	1861	1.76
120	122	1.92	0.19	1861	1.52
122	124	1.90	0.18	1861	1.47

Goebel, 1982). It consists of a deep (15 m) basin toward the southeast and a relatively shallow (1–2 m) northern basin (Fig. 1). The lake is fed by several small first-order streams, which drain the surrounding hills of the small watershed. Presently, the lake drains through a small stream to the NW, but it is closed during drought years. The modern landscape is dominated by agriculture (69% of watershed area), with some remaining stands of oak woodland (22%). Before European settlement, the site was near the prairie-forest ecotone with a mosaic of oak woodland and bigwoods taxa surrounding the lake (Camill et al., 2003). Recent sediments consist of water-rich, massive, gelatinous black mud.

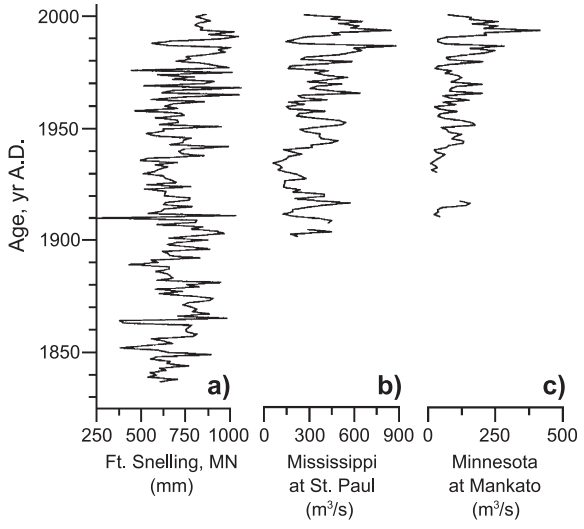

Figure 3. Three precipitation proxies for Sharkey Lake: (a) annual precipitation for Ft. Snelling, MN, (b) mean annual discharge for Mississippi river at St. Paul, MN, and (c) mean annual discharge of Minnesota river at Mankato, MN.

Results and discussion

Figure 4 summarizes the magnetic properties of the shortcore samples. The main results regarding the magnetic record of climate change are:

- A marked increase in the concentration of ferrimagnetic minerals (magnetite, maghemite) during the 1920–1940 drought period as seen in ferrimagnetic susceptibility (κ_{ferri}, Fig. 4d), isothermal remanent magnetization (IRM, Fig. 4e), and S-ratios (Fig. 4g).
- Values of hard IRM (HIRM, Fig. 4f) increase during this period and remain high throughout the remainder of the core, which is due to an absolute increase in high-coercivity minerals.
- Low ratios of ferrimagnetic susceptibility over saturation magnetization (κ_{ferri}/J_S, Fig. 4i) show that 20th century samples are characterized by low concentrations of ultrafine SP magnetite. High ratios of ARM/IRM during drought conditions (1920–1940) suggest a relative increase in fine SD magnetic particles, most likely produced by magnetotactic bacteria.
- Iron oxide minerals in older sediment (pre-1900) are severely affected by the effects of dissolution, leading to a loss in concentration-dependent parameters (κ_{ferri}, IRM, ARM, HIRM) and a bimodal grain size distribution consisting of coarse MD particles (low ratios of ARM/IRM, hysteresis parameters in Fig. 4) and ultrafine SP material (high ratios of κ_{ferri}/J_S, low-T analyses, Fig. 5).

The carriers of the Sediment-magnetic signal

The magnetic mineralogy of Sharkey Lake sediment is characterized by the presence of partially oxidized

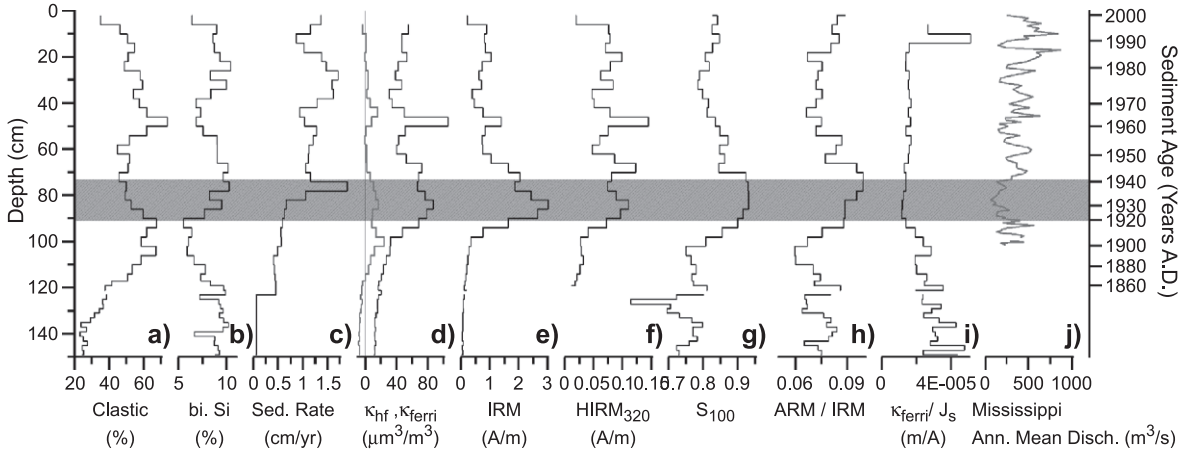

Figure 4. Physical properties of core SHA 02-SC as a function of depth. Corresponding sediment age is shown at the right. (a) Concentration of clastic material and (b) biogenic silica. (c) Sedimentation rates as estimated by ^{210}Pb dating of short-core above 120-cm depth (A.D. 1860) and position of *Ambrosia* rise and ^{14}C dates of long core (SHA 01-A) for samples before 1860. (d) High-field susceptibility κ_{hf} is a proxy for the presence of paramagnetic ($\kappa_{hf} > 0$) or diamagnetic ($\kappa_{hf} < 0$) components, ferrimagnetic susceptibility ($\kappa_{ferri} = \kappa - \kappa_{hf}$) can be used to quantify the abundance of ferrimagnetic minerals. (e) IRM is a proxy for the abundance of ferrimagnetic remanence-carrying ($d > 0.01$ μm) minerals. (f) HIRM estimates the absolute concentration of high coercivity minerals, such as goethite or hematite, while (g) S-ratios are a measure of the relative contribution of these minerals to the magnetic signal. (h) An increase in ARM/IRM ratios implicates a decrease in magnetic grain-size toward smaller SD grains. (i) κ_{ferri}/J_S is a proxy for the presence of ultrafine SP particles. (j) Mean annual discharge of the Mississippi River at St. Paul, MN. Discharge data plotted vs. depth in short-core as estimated from ^{210}Pb age model. Shaded bar highlights the drought during the 1920s to 1940s.

magnetite and ultrafine (less than 30 nm in diameter) superparamagnetic (SP) material. Thermal demagnetization curves (Fig. 5) of magnetic remanence acquired during field-cooling (FC) and zero-field-cooling (ZFC, not shown) to 10 K show a drop in magnetic remanence near 120 K as the samples undergo the Verwey transition, characteristic of (partially oxidized) magnetite (Özdemir et al., 1993). Demagnetization curves for presettlement samples (Fig. 5; Fig. 4b in Geiss et al., 2003) drop significantly at temperatures below 50 K, indicating that a large part of the low-temperature remanence signal is carried by SP minerals. The demagnetization curves of postsettlement samples reveal high concentrations of a ferrimagnetic component unaffected by thermal demagnetization between 10 and 300 K. Increased values of HIRM in the upper 100 cm of the core indicate an increase in the absolute concentration of high-coercivity minerals, such as hematite, goethite, or SD maghemite. Corresponding

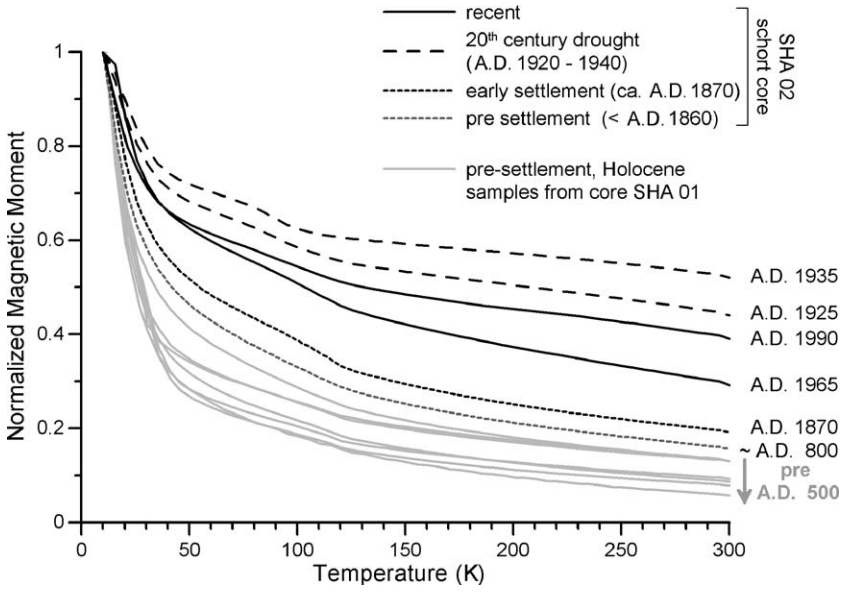

Figure 5. Normalized thermal demagnetization curves of low-temperature magnetic remanence (acquired after field cooling from 300 to 10 K in a field of 2.5 T). All samples show a drop in remanence near 120 K due to the presence of partially oxidized magnetite. The loss in remanence below 50 K is caused by the thermal unblocking of ultrafine, superparamagnetic (SP) iron-bearing minerals. The abundance of SP material increases roughly with sample age as Fe-oxide minerals are progressively dissolved under reducing conditions. Included for comparison are measurements of Holocene samples (Geiss et al., 2003), shown in light gray. Approximate sample ages for each measurement are given at the right side of the figure.

changes in the SP-fraction are also detected by κ_{ferri}/J_S ratios, which are, with the exception of the two uppermost samples, low for samples above the European settlement horizon (Fig. 4i). IRM acquisition curves (Fig. 6) are nearly saturated (>90%) in acquisition fields larger then 300 mT, confirming magnetite/maghemite as the dominating magnetic mineral. Hysteresis measurements (not shown) agree with this interpretation of magnetic mineralogy and show that the bulk-magnetic grain size of all samples falls into the pseudo-single-domain (PSD) grain size range (Fig. 7).

Changes in sediment-magnetic properties through time

Pre-European settlement (pre-A.D. 1860)

These early samples are characterized by low concentrations of magnetic minerals, resulting in low values for concentration-dependent magnetic parameters, such as κ_{ferri} and IRM (Figs. 4d and e). Variable, moderately high ratios of ARM/IRM (<0.8, Fig. 4h) and hysteresis parameters combined with high ratios of κ_{ferri}/J_S (Fig. 4i) indicate a bimodal grain size distribution of relatively coarse (MD to PSD) and ultrafine (SP) magnetic particles. The high abundance of SP particles is confirmed by low-temperature analyses (Fig. 5).

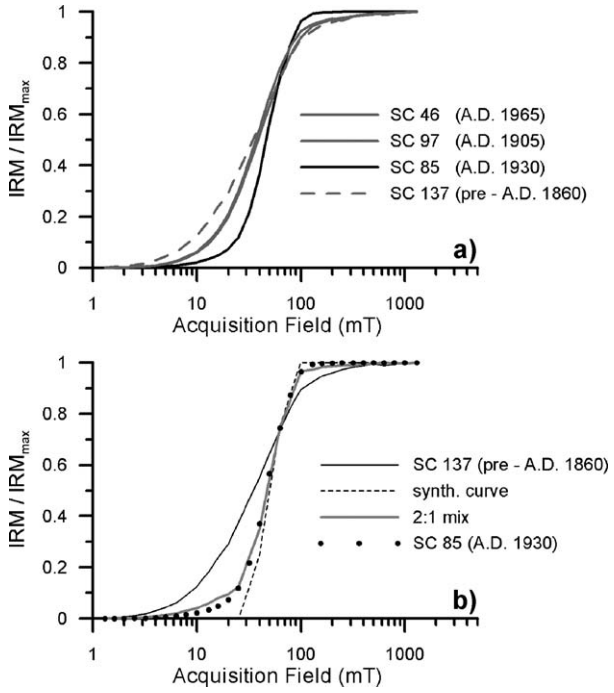

Figure 6. (a) IRM acquisition curves for various samples from SHA 02-SC. Solid gray curves: samples deposited since the onset of Euroamerican settlement. Solid black curve: sample deposited during Dust Bowl drought. Dashed gray curve: presettlement sample. (b) Results of a simple numerical mixing model to simulate the addition of SD bacterial magnetite to a presettlement sample. Solid black curve: presettlement sample, dashed black curve: synthetic SD sample, the resulting mixing curve is shown in gray and provides a good match to measured data from the drought period (solid symbols).

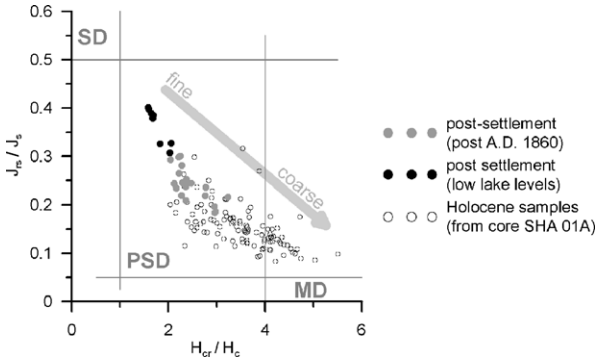

Figure 7. Plot of J_{rs}/J_s vs. H_{cr}/H_c (Day et al., 1977) for samples from Sharkey Lake. Recent samples tend to be finer grained than samples deposited during the Holocene. Samples deposited during low lake levels plot closest to the single-domain (SD) field.

Early settlement (A.D. 1860–1920)

The onset of Euroamerican agriculture and associated increase in erosion rates is reflected in an (slight) initial increase in magnetic susceptibility (κ_{hf}, κ_{ferri}) and IRM (Figs. 4d and e). The magnetic minerals are still fairly coarse grained. A gradual decrease in κ_{ferri}/J_S (Fig. 4i) is interpreted as a decrease in the abundance of SP particles, which is consistent with thermal demagnetization curves (not shown).

20th century drought (A.D. 1920–1940)

Drought conditions are inferred from two decades of low discharge for the Mississippi river (Fig. 4j) and low lake levels, which persisted until the late 1960s due to a gradual recharge of the groundwater table (Fig. 1b). These conditions are reflected in a 3- to 5-fold increase in κ_{ferri} and IRM (Figs. 4d and e), and an increase in the abundance in small SD particles (high ARM/IRM ratios in Fig. 4h). Hysteresis data for this time interval plot closer to the SD field in Figure 7, confirming our interpretation of ARM/IRM ratios. The abundance of ultrafine SP material, however, is low as interpreted from low ratios of κ_{ferri}/J_S (Fig. 4i) and low-T analyses (Fig. 5). HIRM values as high as 0.12 A/m are caused by the addition of high coercivity minerals. The increase of S-ratios during the same interval, however, shows that the relative importance of these minerals decreases, which is due to an even greater input of low-coercivity ferrimagnets.

Recent sediment (past A.D. 1940)

Concentration-dependent parameters such as κ_{ferri} and IRM (Figs. 4d and e) drop slowly and level out at a value approximately five times higher than observed during presettlement. Variable, but lower ratios of ARM/IRM (Fig. 4h) as well as hysteresis measurements (Fig. 7) indicate a slight coarsening of the magnetic fraction, while ultrafine SP grains remain absent (consistently low ratios of κ_{ferri}/J_S), except for the uppermost two samples. The contribution of high-coercivity minerals as estimated from the HIRM record remains high, but S-ratios near 0.8

confirm that the magnetic record is still dominated by low-coercivity ferrimagnets, such as magnetite or maghemite.

The effects of Euroamerican settlement

The rapid conversion of tallgrass prairie and oak savanna to an agricultural landscape within 10–20 yr of the onset of Euroamerican settlement about 1860 (U.S. Bureau of the Census, 1870) led to a significant increase in erosion rates. The resulting increase in the clastic component (Fig. 4a) is reflected in an initially slight increase in concentration-dependent magnetic parameters, such as κ_{ferri} or IRM. Grain size-dependent parameters such as ARM/IRM (Fig. 4h) or hysteresis parameters are variable, but do not indicate a major shift in magnetic grain size. The abundance of ultrafine SP particles decreases as seen in low-temperature analyses (Fig. 5) and low ratios of κ_{ferri}/J_S (Fig. 4i). The rise in concentration-dependent parameters is not solely due to increased erosion rates. Comparing presettlement samples to recent sediment shows that IRM, a good proxy of large remanence carrying ferrimagnetic minerals, increases approximately 10-fold, while the abundance of clastic material only doubles during the same interval (Figs. 4a and e). The marked increase of IRM and other concentration-dependent magnetic parameters in recent sediments is likely due to the combined effects of increased sedimentation rates since settlement and the long-term dissolution of iron-oxide minerals under anoxic conditions, which removes magnetic minerals from presettlement horizons.

20th century drought signal

The discharge record of the Mississippi river (Fig. 4j), which averages over most of Minnesota, shows a marked decrease in precipitation between 1920 and 1940, which led to low lake levels that persisted until the mid-1960s as shown in aerial photographs (Fig. 1b). High values of κ_{ferri} and IRM during this period are superimposed on the anthropogenic erosion signal, but an increase in ARM/IRM ratios (Fig. 4h) and a shift of hysteresis properties toward the SD field in Fig. 7 testifies of the addition of fine-grained SD material. IRM acquisition curves (Fig. 6a) show that the additional component has a very narrow coercivity distribution in the SD size range.

Increased topsoil erosion, which could supply a strongly magnetic, fine-grained component to the lake, is a possible explanation for the observed magnetic signal. However, the concentration of clastic material does not increase during drought conditions, and the concentration of magnetic minerals in the upper horizons of regional soils is too low to explain the observed increases in κ_{ferri} and IRM, given the relatively low abundance of clastic material (Geiss and Umbanhowar, unpublished data). Topsoil within the region is characterized by an accumulation of both SD and SP material, the latter occurring only in low concentrations in the lake sediment.

The tight coercivity distribution mentioned earlier suggests the presence of authigenic magnetite, produced by magnetotactic bacteria (Pósfai et al., 2001). Magnetotactic bacteria are abundant in modern freshwater sediment (e.g., Petersen et al., 1989; Snowball et al., 2002; Spring et al., 1993), and recent studies emphasize their contribution to the sediment magnetic signal (Oldfield and Wu, 2000; Pósfai and Arató, 2000). Higher levels of biogenic silica during this period (Fig. 4b) suggest higher lake productivity, possibly due to increased nutrient supply into a much smaller lake (Fig. 1b). In addition, lower lake levels may have led to better mixing of the water column and better oxygenated bottom conditions, which may have led to better preservation of fine grained iron-oxide minerals. Low rates of dissolution are suggested by the low abundance of SP material (Fig. 5) during periods of low lake levels (Tarduno, 1995).

Addition of a SD component to presettlement material can be simulated with a simple numerical model of IRM acquisition (Fig. 6b). The added component has a coercivity distribution similar to that of samples of magnetotactic bacteria described by Moskowitz et al. (1988) with a mean coercivity of 50 mT, consistent with Egli (2003). Drought samples are about three times as magnetic as other postsettlement samples with comparable concentrations of clastic material. Consequentially, a 2:1 mix between a synthetic SD component and predrought material comes close to reproducing the observed IRM acquisition curves for drought samples. Addition of bacterial SD magnetite with a narrow grain size distribution is in agreement with relatively high ARM/IRM ratios as well as the shift toward the SD field observed in Figure 7.

The magnetic signal described above persists for at least a decade after the 1940s drought, which suggests that it is at least partly controlled by low lake levels rather than precipitation or vegetation change.

The modern sediment-magnetic record as an analog for mid-Holocene drought

At Sharkey Lake, droughts during the mid-Holocene caused a distinct change in vegetation from oak savanna to prairie between 8500 and 4000 yr ago (Camill et al., 2003), which led to increased detrital input into the lake either due to soil erosion or eolian deposition. These changes are reflected in the sediment-magnetic record as an increase in magnetic minerals, as well as a shift to coarser magnetic grain sizes (Geiss et al., 2003).

During the 20th century, the sedimentary record of climate change is severely disturbed by anthropogenic activities, and any climate signal is superimposed on an anthropogenic erosion signal. In addition, drought conditions during the Dust Bowl period were not severe enough in Minnesota to cause significant shifts in vegetation and dune remobilization (Keen and Shane, 1990). Areas of wind erosion and dust storm tracks were

limited mainly to the southwestern United States (Cunfer, 2002; Cunfer, personal communication 2003), making large-scale eolian deposition unlikely. Sediment deposited during this period is characterized by a magnetic background signal from clastic material and the addition of an autochthonous SD-sized magnetite, resulting in high concentrations of magnetic minerals and a shift to fine SD magnetic particles.

Long-term dissolution of Fe-oxide minerals under reducing conditions can explain these seemingly contradictory results. As pointed out by Geiss et al. (2003), autochthonous biogenic magnetite is the predominant magnetic component in the lake during humid periods, but may have played a significant role throughout the Holocene. Our new short core data confirm this model and stress the importance of dissolution processes as a filter on the magnetic signal. Both modern and mid-Holocene samples consist of approximately 50% clastic material, however, maximum IRM-values for the mid-Holocene reach only 0.3 A/m (Geiss et al., 2003) compared to 1 to 2 A/m in modern samples (Fig. 4e). Assuming a clastic source with similar magnetic properties, it is evident that 60–80% of the original IRM signal has been lost. Because dissolution is a surface process, it affects small grains with high surface/volume ratios first and leads to an apparent coarsening of the magnetic component toward MD particles, provided that such large grains are initially present. This increase in average grain size is reflected in a shift of presettlement samples toward the MD field in Figure 7. Part of the dissolved Fe may remain in the sediment and lead to the formation of a nanosized, SP component as observed in the older samples of Sharkey Lake. The addition of SP material can cause a similar shift toward the MD field in Figure 7. A coarsening of the magnetic grain size, however, is also indicated by lower ARM/IRM ratios that are independent of SP contributions. Our magnetic data indicate a bimodal grain size distribution of SP and MD magnetic particles for these older sediments. Such bimodal grain size distributions have been observed in pelagic sediments (Tarduno, 1995), where they are also associated with the dissolution of iron minerals under reducing conditions. Early Holocene dry periods are characterized by coarse grained magnetic material because they received a combination of SD and MD particles and lost the SD component due to post depositional dissolution of iron-oxide minerals, leading to a bimodal distribution of SP and MD grains. Sediments deposited during humid time periods were initially characterized by authigenic SD magnetic particles. They also underwent postdepositional dissolution leading to extremely low concentrations of magnetic minerals in the SP to SD grain size range. Recent samples are characterized by the large erosional influx due to Euroamerican agriculture regardless of climate and are too young for significant postdepositional dissolution to occur. In these sediments, higher organic productivity leads to decreases in mean magnetic grain size during dry periods as shown in Figure 4. These modern samples therefore make poor modern analogs for the interpretation of older records, but their study can shed light on the long-term fate of iron oxide minerals and aid in the interpretation of older records in terms of paleoenvironmental change.

Conclusions

The onset of European style farming led to increased erosion rates that are reflected in the sediment-magnetic properties as an increase in concentration-dependent parameters such as magnetic susceptibility (κ) or isothermal remanent magnetization (IRM). Episodes of drought led to lower lake levels and higher lake productivity. These result in the addition of a fine-grained, single-domain magnetic component with a narrow coercivity range, which is most likely produced by magnetotactic bacteria and leads to an increase in the concentration of magnetic minerals and a shift toward finer particle size distributions. This shift is shown by high ratios of ARM/IRM as well as hysteresis data.

The magnetic drought signal recorded during the 20th century Dust Bowl, however, persisted for more than two decades after the end of drought conditions, as the lake slowly reached its predrought levels. This indicates that the magnetic signature of drought conditions is probably linked to lower lake levels rather than precipitation.

Upon deposition in a predominantly anoxic environment, iron oxide minerals are affected by dissolution, which over time, leads to decreasing concentrations of magnetic minerals and the development of a bimodal grain size distribution of ultrafine, superparamagnetic, and large, multidomain grains.

A comparison between modern and mid-Holocene samples shows that the magnetic properties of modern samples yield poor direct analogs of past environments, even though the processes that caused the initial magnetic signal are likely similar. This is due to the superposition of climatic and anthropogenic influences on the sediment magnetic record and the effects of long-term dissolution, which act as a filter on the magnetic properties of older sediment. These constraints are probably not limited to lake sediment, but to any depositional environment, which is at least temporarily affected by anoxia (e.g., soils). Studies based mainly on one single magnetic parameter, such as magnetic susceptibility, run the severe risk of misinterpreting the magnetic record.

However, magnetic analyses of lake sediment and soil can be a valuable tool for the reconstruction of past environments because it is relatively independent of most other paleoclimate proxies. This study shows that a careful characterization of the magnetic component can recognize postdepositional changes, and a multi-proxy magnetic study can yield valuable information regarding past environmental conditions.

Acknowledgments

We thank Margaret Sharkey for generous access to the site. The magnetic analyses were performed at the Institute for Rock Magnetism, which is funded by the W.M. Keck Foundation, the NSF Earth Sciences Division's Instrumentation and Facilities Program, and the University of Minnesota. Part of this study was funded by NSF/ATM grant 9909523 and grants by the Howard Hughes Medical Institute to Carleton and St. Olaf Colleges. L. Dvorak, J. Aldinger, and K. Walkup performed analyses of biogenic silica. The comments of S. Colman and an anonymous reviewer helped to greatly improve the manuscript. We thank Greg Spoden, MN State Climatology Office, for providing us with the unpublished climate data for Ft. Snelling, MN.

References

Binford, M.W., 1990. Calculation and uncertainty analysis of ^{210}Pb dates for the PIRLA project lake sediment cores. Journal of Paleolimnology 3, 253–267.

Camill, P., 1999. Peat accumulation and succession following permafrost thaw in the boreal peatlands of Manitoba, Canada. Ecoscience 6, 592–602.

Camill, P., Lynch, J.A., Clark, J.S., Adams, J.B., Jordan, B., 2001. Changes in biomass, aboveground NPP, and peat accumulation following permafrost thaw in the boreal peatlands of Manitoba, Canada. Ecosystems 4, 461–478.

Camill, P., Umbanhowar, C.E., Teed, R., Geiss, C.E., Dvorak, L., Kenning, J., Limmer, J., Walkup, K., Aldinger, J., 2003. Late-glacial and Holocene climatic effects on fire and vegetation dynamics at the prairie-forest ecotone in south-central Minnesota. Journal of Ecology 91, 822–836.

Conley, D.J., 1998. An interlaboratory comparison of the measurement of biogenic silica in sediments. Marine Chemistry 63, 39–48.

Cunfer, G., 2002. Causes of the dust bowl. In: Knowles, A.K. (Ed.), Past Time, Past Place, GIS for History. ESRI Press, Redlands, CA, pp. 93–104.

Day, R., Fuller, M., Schmidt, V.A., 1977. Hysteresis properties of titanomagnetites: grain-size and compositional dependence. Physics of the Earth and Planetary Interiors 13, 260–267.

Dean, W.E., 1974. Determination of carbonate and organic matter in calcareous sediments and sedimentary rocks by loss on ignition: comparison with other methods. Journal of Sedimentary Petrology 44, 242–248.

Eakins, J.D., Morrison, R.T., 1978. A new procedure for the determination of ^{210}Pb in lake and marine sediments. International Journal of Applied Radiation and Isotopes 29, 531–536.

Egli, R., 2003. Analysis of the field dependence of remanent magnetization curves. Journal of Geophysical Research 108, 2081.

Gedye, S.J., Ammann, B., Oldfield, F., Jones, R.T., Tinner, W., 2000. The use of mineral magnetism in the reconstruction of fire history: a case study from Lago di Origlio, Swiss Alps. Palaeogeography, Palaeoclimatology, Palaeoecology 164, 101–110.

Geiss, C.E., Umbanhowar, C.E., Camill, P., Banerjee, S.K., 2003. Sediment magnetic properties reveal Holocene climate change along the Minnesota prairie-forest ecotone. Journal of Paleolimnology 30, 151–166.

Hobbs, H.C., Goebel, J.E., 1982. Geologic map of Minnesota, Quaternary Geology, Map S-1. Minnesota Geological Survey, St. Paul.

Housen, B.A., Banerjee, S.K., Moskowitz, B.M., 1996. Low-temperature magnetic properties of siderite and magnetite in marine sediments. Geophysical Research Letters 23, 2843–2846.

Hunt, C.P., Banerjee, S.K., Han, J., Solheid, P.A., Oches, E., Sun, W., Liu, T., 1995. Rock-magnetic proxies of climate change in the loess-paleosol sequences of the western loess plateau of China. Geophysical Journal International 123, 232–244.

Keen, K.L., Shane, L.C.K., 1990. A continuous record of Holocene eolian activity and vegetation change at Lake Ann, east-central Minnesota. Geological Society of America Bulletin 102, 1646–1657.

Laird, K.R., Fritz, S.C., Maasch, K.A., Cumming, B.F., 1996. Greater drought intensity and frequency before AD 1200 in the Northern Great Plains, USA. Nature 384, 552–554.

Moskowitz, B.M., Frankel, R.B., Flanders, P.J., Blakemore, R.P., Schwartz, B.B., 1988. Magnetic properties of magnetotactic bacteria. Journal of Magnetism and Magnetic Minerals 73, 273–288.

Oldfield, F., Wu, R., 2000. The magnetic properties of the recent sediments of Brothers Water, N.W. England. Journal of Paleolimnology 23, 165–174.

Oldfield, F., Mercuri, A.M., Juggins, S., Langone, L., Rolph, T., Trincardi, F., Wolff, G., Gibbs, Z., Vigliotti, L., Frignani, M., Van der Post, K., Branch, N., Asioli, A., Accorsi, C.A., 2003. A high resolution late Holocene palaeo environmental record from the central Adriatic Sea. Quaternary Science Reviews 22, 319–342.

Özdemir, Ö., Dunlop, D.J., Moskowitz, B.M., 1993. The effect of oxidation on the Verwey transition in magnetite. Geophysical Research Letters 20, 1671–1674.

Petersen, N., Weiss, D., Vali, H., 1989. Magnetotactic bacteria in lake sediments. In: Lowes, F. (Ed.), Geomagnetism and Paleomagnetism. Kluwer Academic Publishers, Dordrecht, pp. 231–241.

Pósfai, M., Arató, B., 2000. Magnetotactic bacteria and their mineral inclusions from Hungarian freshwater sediments. Acta Geologica Hungarica 43, 463–476.

Pósfai, M., Buseck, P.R., Frankel, R.B., Bazylinski, D.A., Cziner, K., Márton, E., Márton, P., 2001. Crystal-size distributions and possible biogenic origin of Fe sulfides. European Journal of Mineralogy 13, 691–703.

Reynolds, R.L., Rosenbaum, J.G., Rapp, J., Colman, S.M., 1997. Use of sediment grain size to establish the glacial origin of magnetic property variations at Upper Klamath Lake, OR. EOS 78, F170.

Rochette, P., Fillion, G., Mattei, J.L., Dekkers, M.J., 1990. Magnetic transition at 30–34 Kelvin in pyrrhotite: insight into a widespread occurrence of this mineral in rocks. Earth and Planetary Science Letters 98, 319–328.

Rosenbaum, J.G., Reynolds, R.L., Adam, D.P., Drexler, J., Sarna-Wojcicki, A.M., Whitney, G.C., 1996. A middle Pleistocene climate record from Buck lake, Cascade range, southern Oregon—Evidence from sediment magnetism, trace-element geochemistry, and pollen. Geological Society of America Bulletin 108, 1328–1341.

Snowball, I., Zillén, L., Sandgren, P., 2002. Bacterial magnetite in Swedish varved lake-sediments: a potential bio-marker of environmental change. Quaternary International 88, 13–19.

Spring, S., Amann, R., Ludwig, W., Schleifer, K.H., Van Gemerden, H., Petersen, N., 1993. Dominating role of an unusual magnetotactic bacterium in the microaerobic zone of a freshwater sediment. Applied and Environmental Microbiology 59, 2397–2403.

Stokes, S., Swinehart, J.B., 1997. Middle- and late-Holocene dune reactivation in the Nebraska Sand Hills, USA. Holocene 7, 263–272.

Tarduno, J.A., 1995. Superparamagnetism and reduction diagenesis in pelagic sediments: enhancement or depletion? Geophysical Research Letters 22, 1337–1340.

U.S. Bureau of the Census, 1870. Population Schedules of the Ninth Census of the United States. National Archives Microfilm Publications, No. 593, Washington, DC.

U.S. Geological Survey, 2003. Calendar year streamflow statistics for Minnesota, available at: http://waterdata.usgs.gov/mn/nwis/annual.

Verwey, E.J., Haayman, P.W., Romeijn, F.C., 1947. Physical properties and cation arrangement of oxides with spinel structures: II. Electronic conductivity. Journal of Chemical Physics 15, 181–189.

Wright Jr., H.E., 1992. Patterns of Holocene climatic change in the Midwestern United States. Quaternary Research 38, 129–134.